

Supplementary Information

Carboxylic Ester-Terminated Fullero pyrrolidine as an Efficient Electron Transport Material for Inverted Perovskite Solar Cells

Junwei Chang,^{†,a,b} Ying-Chiao Wang,^{†,b} Changjian Song,^{b,c} Liping Zhu,^b Qiang Guo,^a

Junfeng Fang^{*,b,c}

^aDepartment of Polymer Materials, School of Materials Science and Engineering, Shanghai University, Nanchen Road 333, Shanghai 200444, China

^bKey Laboratory of Graphene Technologies and Applications of Zhejiang Province, Ningbo Institute of Materials Technology and Engineering, Chinese Academy of Sciences, Ningbo 315201, China

^cUniversity of Chinese Academy of Sciences, Beijing 100049, China

[†]These authors contributed equally to this work

*Correspondence and requests for materials should be addressed to J.F. (email: fangjf@nimte.ac.cn).

EXPERIMENTAL DETAILS

Materials and device fabrication

Poly(3-(4-carboxylbutyl) thiophene) (P3CT) (Rieke, America) solutions (1 mg of P3CT in 1 mL methanol) are spin-coated on the clean ITO glass ($R_S \leq 15 \Omega \text{ sq}^{-1}$) at 4000 rpm for 30 s to fabricate a thin P3CT HTL. Then, perovskite precursor solutions (1.45 M in a N, N-dimethylformamide/dimethyl sulfoxide co-solvent with a 1:1 molar ratio of PbI_2 to methylammonium iodide ($\geq 99.5\%$) (Xi'an Polymer Light Technology Corp.)) are deposited on the ITO/ P3CT templates in a glovebox by spin-coating at 4800 rpm for 20 s with a chlorobenzene (CB) treatment 8 s after the spin-coating begins. After that, the films are annealed at 60 °C for 20 s and at 80 °C for 2 minutes. Solutions of CPTA-E (Sigma-Aldrich, 97%) in chlorobenzene: chloroform (CF) co-solvent with a volume ratio of 1:1 are prepared with a concentration of 5 (30 nm), 10 (50 nm), 15 (70 nm) and 20 mg mL^{-1} (90 nm). The annealed perovskite films are covered by the CPTA-E solutions at 2000 rpm for 60 s, followed by the deposition of 70 nm patterned Al top electrodes by thermal evaporation. The P3CT and perovskite precursor solutions are filtered through a 0.45 μm polytetrafluoroethylene filter prior to use.

Characterization and measurements

The cross-sections of devices are observed by scanning electron microscopy (SEM) (S4800, Hitachi, Japan). Ultraviolet photoelectron spectroscopy (UPS) measurements and X-ray photoelectron spectroscopy (XPS) measurements are carried out using a Kratos AXIS ULTRA DALD XPS/UPS system. The UPS measurements are conducted by Shimadzu Spectrometer (AXIS ULTRA DLD) with a He I (21.2

eV) discharge lamp. The photocurrent density-voltage characteristics (Keithley 2410 source meter) are measured using a calibrated solar simulator (Newport Inc.) with an AM 1.5G filter under an irradiation intensity of 100 mW cm⁻². The external quantum efficiency measurement is conducted with a Newport quantum efficiency measurement system (ORIEL IQE 200TM) combined with a lock-in amplifier and a 150 W Xe lamp in the ambient atmosphere. The light intensity at each wavelength is calibrated by a standard Si/Ge solar cell. Top-view SEM (S4800, Hitachi, Japan) and atomic force microscopy are performed to observe the surface morphology of the CPTA-E and PCBM ETL. XPS survey scans are collected to identify the overall surface composition using a monochromatic Al K α X-ray source (1486.6 eV). High-resolution scans are obtained at a 20 eV pass energy and a 50 meV channel width to identify the bonding states. Photoluminescence spectra are analyzed using a fluorescence spectrophotometer (F-4600, Hitachi Ltd., Tokyo, Japan) with a 150 W Xe lamp as the excitation source at room temperature. Ultraviolet-visible absorption spectra is recorded on a GS54T spectrophotometer (Shanghai Lengguang Technology Co., China). The mobilities (μ) of CPTA-E and PCBM are evaluated with the Mott-Gurney law, given by the equation: $J=9\varepsilon_0\varepsilon_r\mu V^2\exp(0.89\beta(V/L)^{0.5})/(8L^3)$, where J stands for the current density, ε_0 is the permittivity of free space, ε_r is the relative permittivity of the medium (assuming that 3.4), V is the effective voltage, L is the thickness of the active layer and β is the field activation factor.

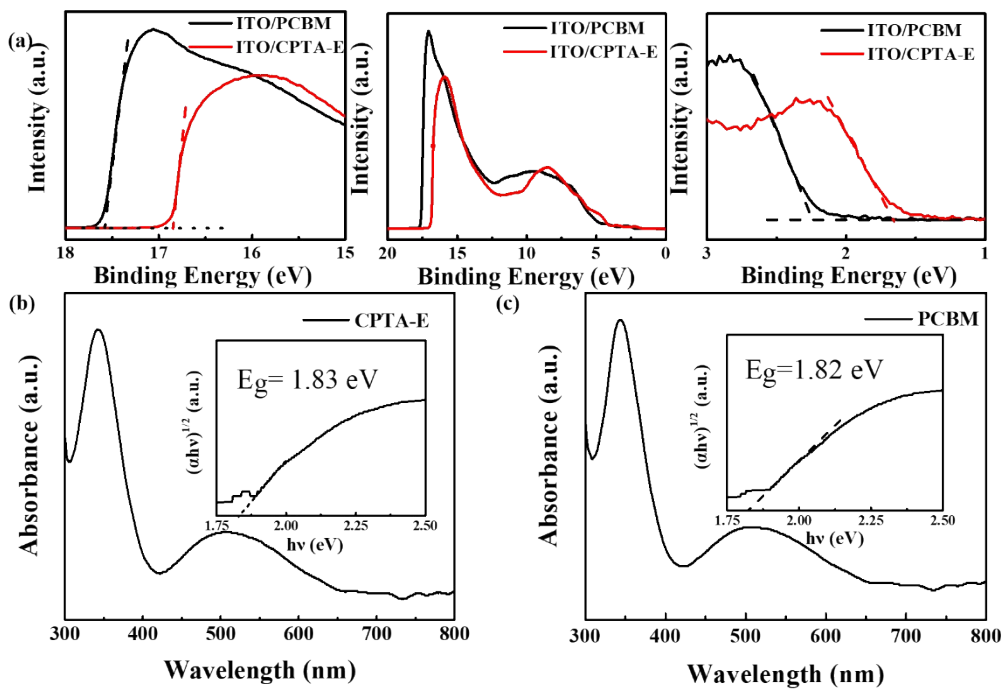


Fig. S1 (a) UPS of CPTA-E and PCBM ETM. The center is the full UPS spectra. The left is the secondary-electron cut-off. The right is the valence-band region. UV-vis absorption spectra of the CPTA-E (b) and PCBM film (c). The insets are the Tauc plots and the corresponding band gap of these two materials.

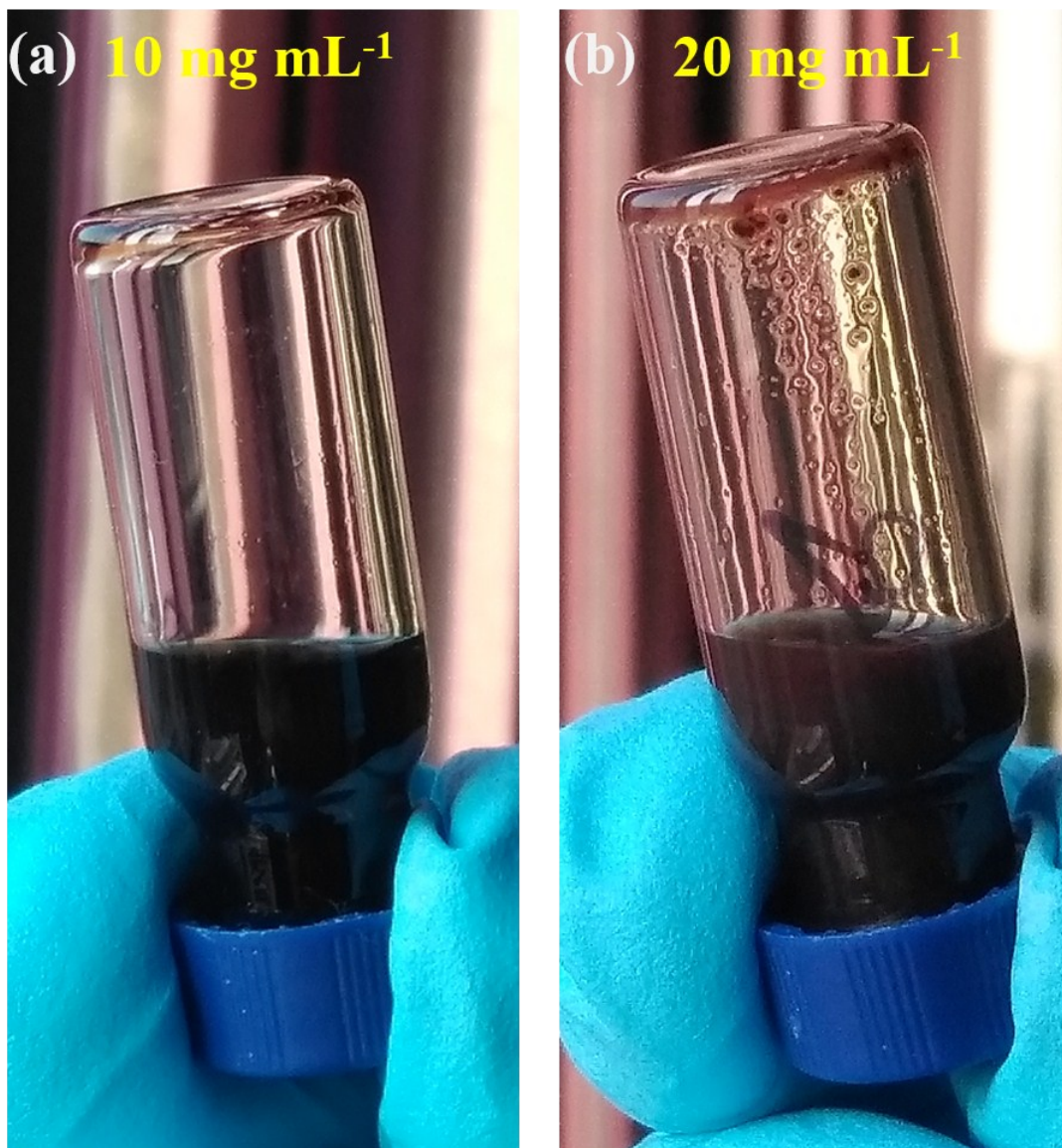


Fig. S2 Photographic images of CPTA-E solutions with a concentration of (a) 10 mg mL⁻¹ and (b) 20 mg mL⁻¹ in CB:CF co-solvent, respectively. Compared with the 10 mg mL⁻¹ CPTA-E solution (Figure S2a), the 20 mg mL⁻¹ CPTA-E solution (Figure S2b) becomes opaque with some aggregations.

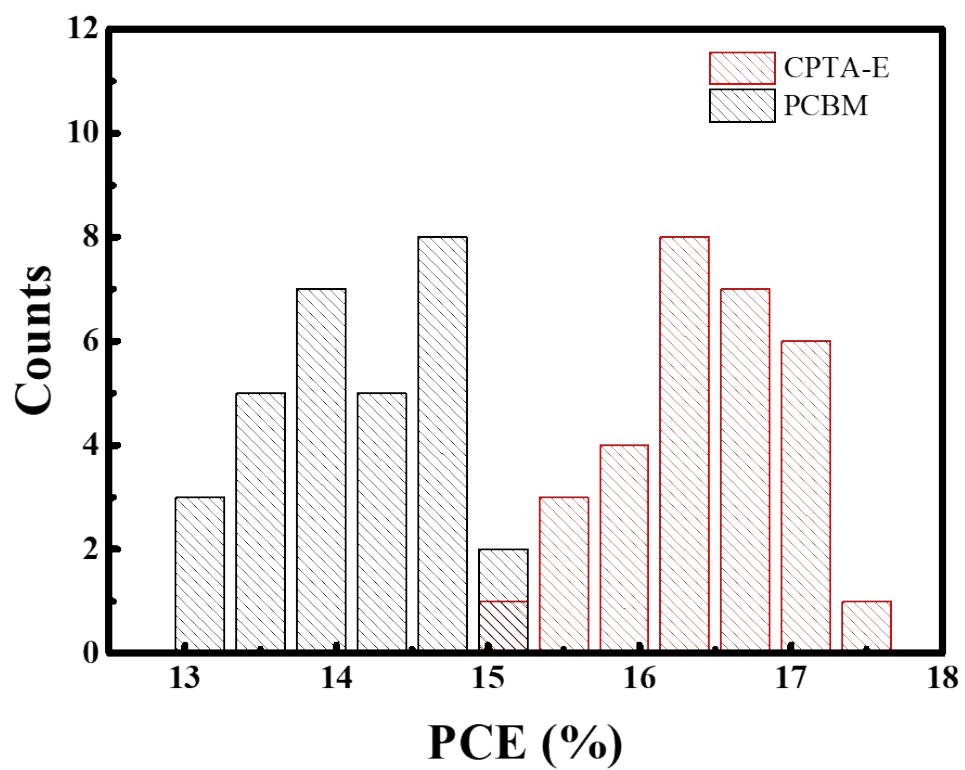


Fig. S3 Histograms of device PCEs measured from 30 identical devices from 5 batches.

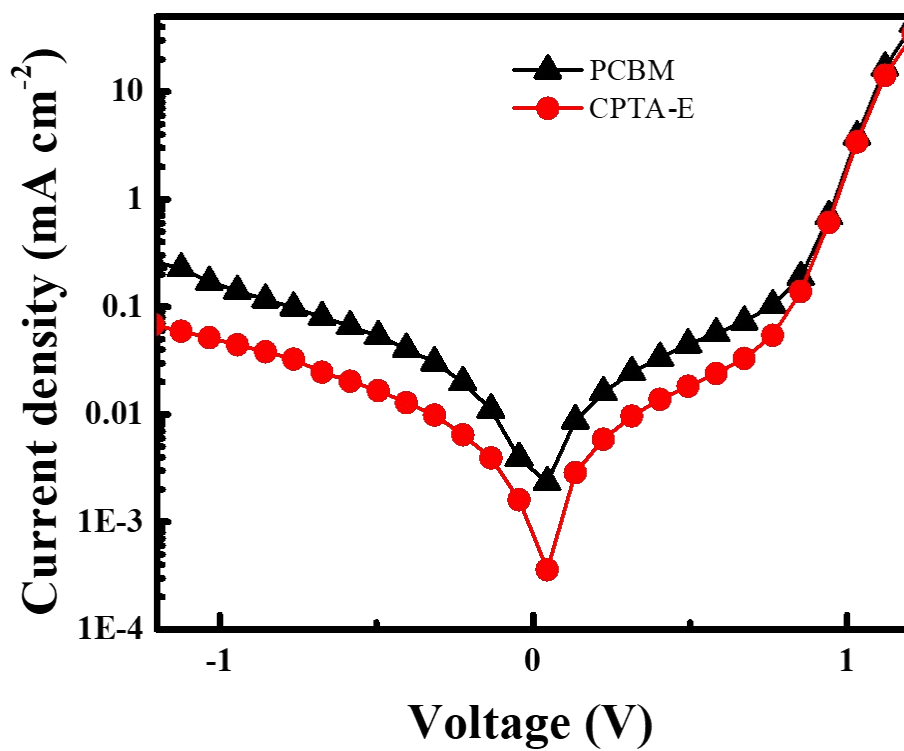


Fig. S4 Logarithmic plots of J - V characteristics of devices with the CPTA-E and PCBM ETL under dark.

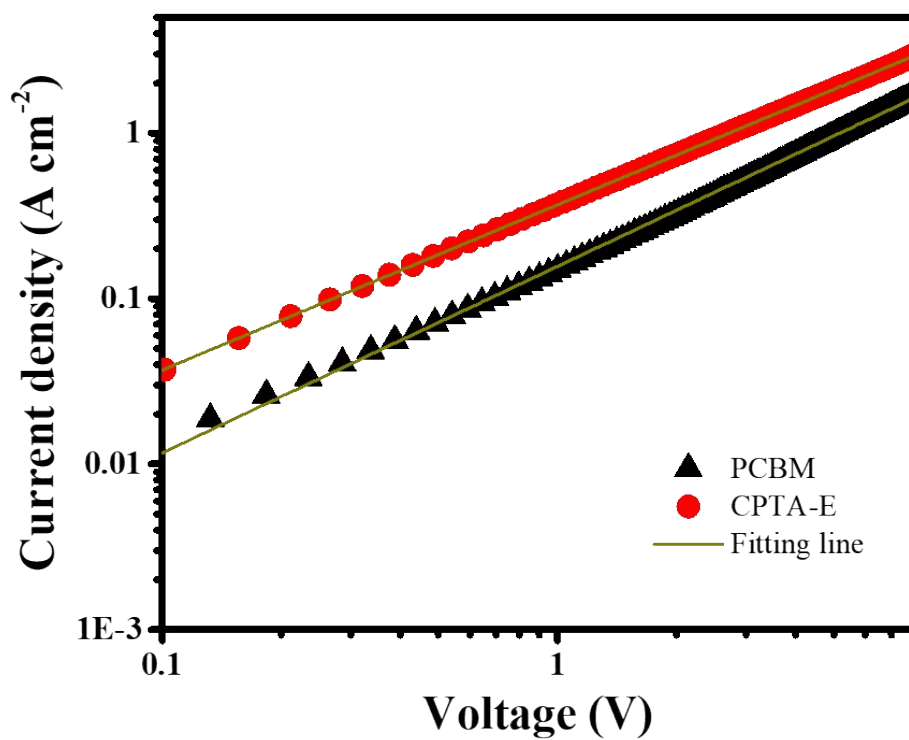


Fig. S5 J - V characteristics of the electron-only devices based on the CPTA-E and PCBM ETL with a structure of ITO/ZnO/ETL/ZnO/Al.

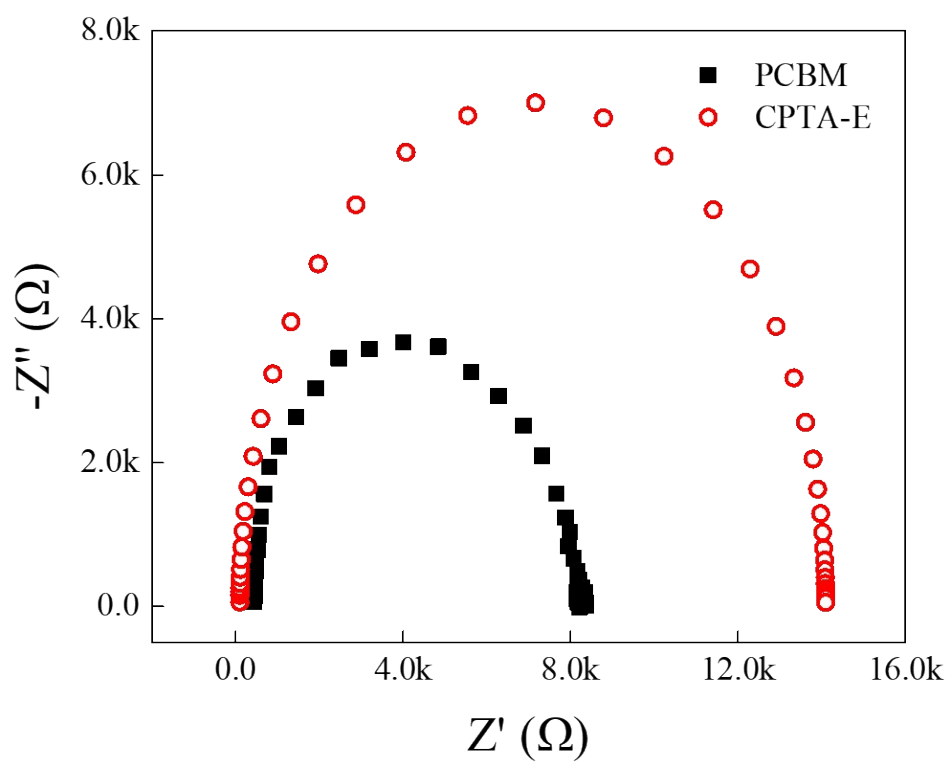


Fig. S6 Alternating current impedance spectrometry (ACIS) of PSCs devices based on CPTA-E and PCBM ETL under dark.

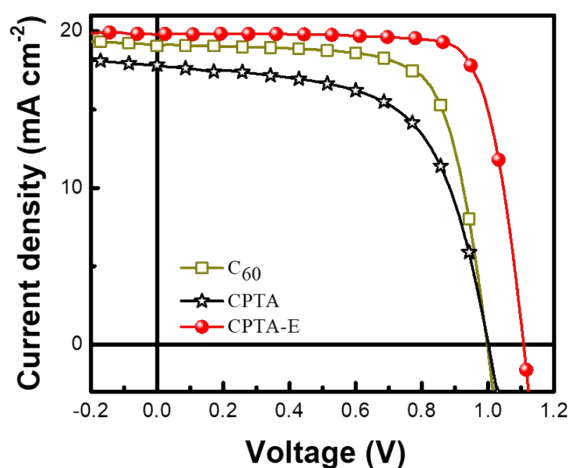


Fig. S7 J - V curves of the perovskite solar cells devices with the C_{60} , CPTA and CPTA-E ETL under AM 1.5 G illumination (100 mW cm^{-2}).

Table S1 Photovoltaic parameters of devices with the C_{60} , CPTA and CPTA-E ETL under AM 1.5 G illumination (100 mW cm^{-2}).

ETL	V_{OC} (V)	J_{SC} (mA cm^{-2})	FF (%)	PCE (%)
C_{60}	0.996	19.16	71.70	13.69
CPTA	0.999	17.79	61.43	10.93
CPTA-E	1.106	19.80	78.08	17.10

Perovskite solar cells with C_{60} ETL show a PCE of 13.69%, a V_{OC} of 0.99 V and a FF of 71.70%. We think that the unsuitable energy level of C_{60} lead to the inferior performance. The LUMO energy level is about -4.5 eV from previous reports, leading to inevitably energy loss at perovskite/ETL interface. The CPTA based device shows a relatively low power conversion efficiency (PCE) than CPTA-E based device. The reasonable explanation might be that CPTA has a worse solubility in chlorobenzene:

chloroform solvent. Therefore, the spin-coated CPTA ETL has a rough surface and poor contact with perovskite, which result in the low J_{SC} , FF and PCE.

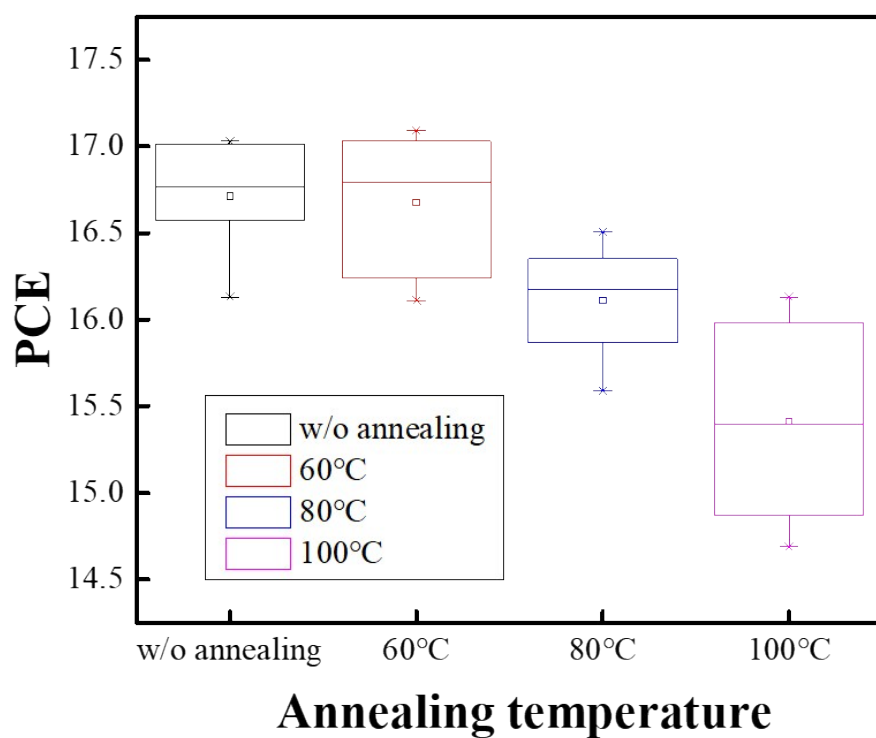


Fig. S8 Statistic photovoltaic parameters of different CPTA-E annealing temperature.

As shown in Figure S7, 60°C annealing scarcely changed the devices performance. But when the annealing temperature rose to 80°C, PCE of the devices began to decreased. After 100°C annealing, the PCE showed considerable decline. These results indicate that high temperature over 80°C could decompose the structure of perovskite, leading to the decrease of devices performance.

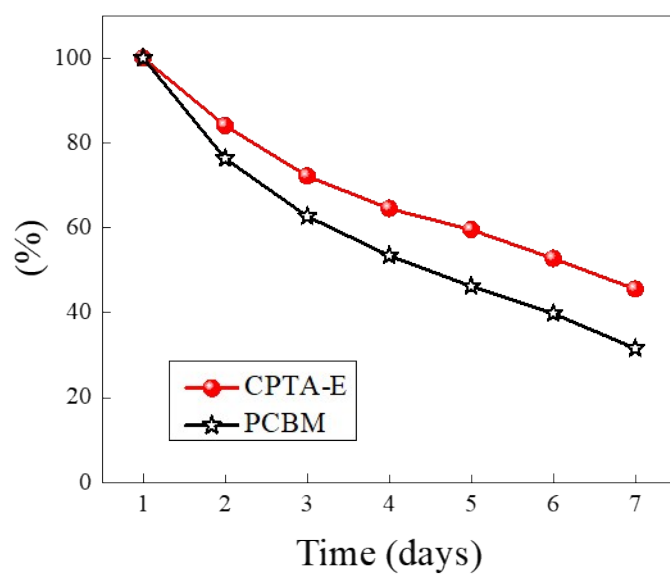


Fig. S9 Evolution of normalized PCE of CPTA-E and PCBM based perovskite solar cells in ambient conditions (about 50% RH). After storing in air for seven days, both of PCE of these two devices decreased to lower than 50% of their pristine PCE. The air instability of these devices might result from the hygroscopicity of the thin P3CT HTL. As shown in Fig. S8, the CPTA-E based device has a better air stability than the PCBM one, which is contributed to the relatively dense and compact CPTA-E ETL.

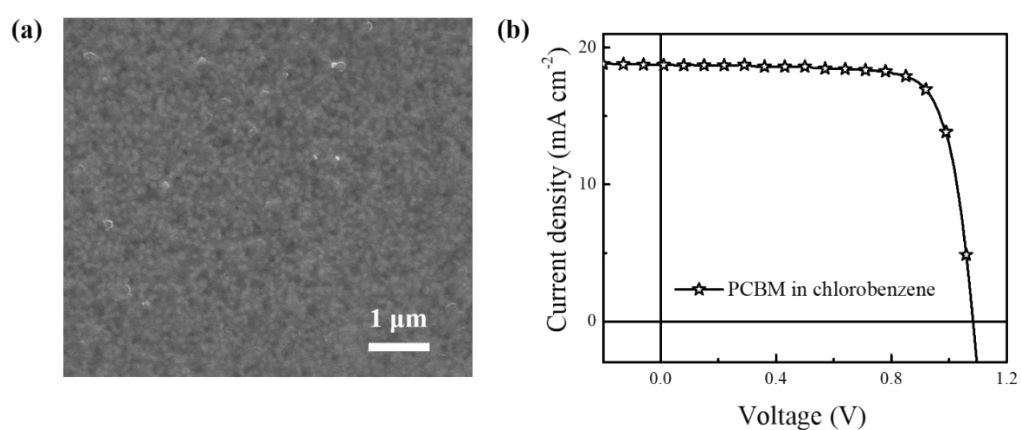


Fig. S10 (a) Top-view SEM image of PCBM film spin-coated from chlorobenzene solvent. (b) Corresponding J - V curve of the PCBM based device. The PCBM film made from chlorobenzene solvent has less pinholes. Compared to the PCBM film made by chlorobenzene: chloroform hybrid solvent, the PCBM film made from chlorobenzene solvent has less pinholes. The perovskite device with PCBM ETL shows a PCE of 15.6% with a V_{OC} of 1.082 V, a J_{SC} of 18.73 mA cm⁻² and a FF of 77.11%. Though the numbers of pinholes of PCBM film is reduced, the PCE of PCBM based device (15.6%) is still lower than the CPTA-E based device (17.44%).

Table S2 Photovoltaic parameters of PCBM device fabricated from chlorobenzene solvent under AM 1.5 G illumination (100 mW cm⁻²).

ETL	V_{OC} (V)	J_{SC} (mA cm ⁻²)	FF (%)	PCE (%)
PCBM	1.082	18.73	77.11	15.60

Reference

1. J. Y. Jeng, Y. F. Chiang, M. H. Lee, S. R. Peng, T. F. Guo, P. Chen and T. C. Wen, *Adv. Mater.*, 2013, **25**, 3727-3732.
2. X. Li, X. Liu, X. Wang, L. Zhao, T. Jiu and J. Fang, *J. Mater. Chem. A.*, 2015, **3**, 15024-15029.